SOLVING SO_2 DISPERSION FROM COMBUSTION FLUE GAS USING PLUME REFLECTION ON THE GROUND FOR CONTINUOUS POINT SOURCE MODEL

Dana-Cristina TONCU[1], Alina BOGOI[2], Virgil STANCIU[3], Sterian DANAILA[4]

În această lucrare se prezintă calculul concentraţiei maxime de SO_2 la sol şi al distanţei, pe direcţia vântului, la care concentraţia este maximă, pentru gazele de coş pentru cuptoarele din industria de prelucrare a petrolului cu modelul penei, cu sursă punctiformă continuă, reflectată.

In this study, SO_2 maximum ground concentration and the distance, on wind direction, at which SO_2 ground concentration is maximum are presented, for the case of combustion flue gas released by a petroleum industry furnace using plume reflected virtual continuous point source dispersion model.

Keywords: SO2 dispersion, combustion gas, diffusion equation, numerical solution.

1. Introduction

Air pollution is a major environmental problem affecting the whole world. The prevalence of increasingly high levels of atmospheric pollutants, particularly sulfates, especially over industrial regions, has received the required attention, becoming research subject studying its causes, nature and effects. Also, the release of sulpfur compounds by power plants and industrial complexes has gained particular concern, mainly due to their conversion. Substantial SO_2 amounts are believed to result from long-range transport lasting one or more days.

Numerous efforts were done to develop mathematical models to simulate long range SO_2 transport, from steady-state models to regional ones, such as large plumes dispersed throughout the mesoscale layer and contacting ground, in which source height and emission rate determine pollutant distribution. Strong stability preserving properties of Runge-Kutta time discretization methods were developed

[1] PhD. student, Dept. of Aerospace Engineering, University POLITEHNICA from Bucharest, România, e-mail: cristinatoncu@canals.ro
[2] Lecturer, Dept. of Aerospace Engineering, University POLITEHNICA from Bucharest, România, e-mail: bogoi_alina@yahoo.com
[3] Professor, Dept. of Aerospace Engineering, University POLITEHNICA from Bucharest, România, e-mail: vvirgilstanciu@yahoo.com
[4] Professor, Dept. of Aerospace Engineering, University POLITEHNICA from Bucharest, România, e-mail: sdanaila@gmail.com

[1], finite difference schemes were improved for evaluating high order derivatives [2], most of the previous studies focused on passive gas dispersion [4], while source and transport approaches tried to better fit prediction [5]. Few 3-dimensional advection-diffusion equations of air pollution were solved [6], some of them by using cubic spline interpolation [7].

Diagnostic plume models aim to correctly identify and characterize pollutant emission and transmission. The goal of this paper is to use the diffusion plume model in an integrated phenomenological-mathematical research. The specific objectives of such an approach are: identification of the best calculus method for SO_2 concentration from combustion flue gas and 3-D representation of SO_2 concentration.

2. Problem formulation

Usually, combustion inside furnace is complete and thus there is no CO in combustion gas. In the case of fuels containing sulfur, combustion gas encloses SO_2, which is its main noxious constituent.

Due to inertia, combustion gas initially has an ascendant motion when evacuated, and then is taken by wind, on its direction, still occurring horizontal and vertical dispersion.

Combustion gas elevation above furnace is given by the following equation [3]:

$$\Delta h = \frac{1{,}9 \cdot D \cdot \omega}{\omega_{10} \cdot (0{,}1 \cdot h_c)^{\frac{n}{2-n}}} \tag{1}$$

in which: D – inner furnace diameter (at the top), m; ω – speed of burnt gas at the top of the furnace, m/s; ω_{10} – wind speed at 10 m above ground, m/s; h_c – quotation of top of furnace, m; n – turbulence index for air.

It is recommended to use in calculus $\omega_{10} = 2...3 m/s$, taking into account that higher speed favors dispersion.

Turbulence index depends upon atmospheric state, and is already mentioned in literature.

It is recommended to use for such calculus $n = 0.25$, which corresponds to stable atmospheric state.

The altitude at which dispersion starts has the value [3]:

$$h_d = h_c + \Delta h \tag{2}$$

Evacuated flow of SO_2 through combustion gas is given by [3]:

$$Q_{SO_2} = \frac{M_{SO_2}}{M_S} B \cdot s = 2 \cdot B \cdot s \tag{3}$$

in which: B – fuel mass, kg/h; s – sulfur mass fraction in fuel.

2.1. Diffusion equation

Most mathematical models are based on two important representations: puff and plume diffusion. Both of them are taking into account mass balance equation and the source type. In this paper, a continuous injection in uniform flow is used to correspond to furnace, from time $t=0$ to the current time t. Fig.1 shows the graphical representation for the plume model, with coordinates' origin at furnace bottom, wind in x-direction and gas flow (plume) rising from the source, moving on $0x$ and spreading both $0x$ and $0y$ directions.

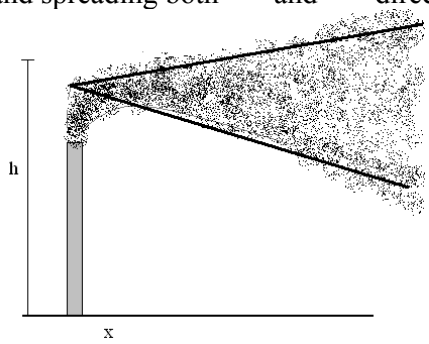

Fig.1. Graphical representation of plume dispersion model

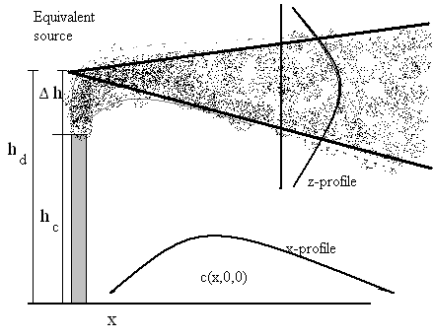

Fig.3. Scheme of the used approach

2.2. The turbulent advection-diffusion equation

In order to derive an advection-diffusion equation for turbulence, the Reynolds decomposition is substituted into the normal equation for advection-diffusion. The Reynolds decomposition analogy for the concentration is [5]:

$$c(\mathbf{x},t)=\overline{c}(\mathbf{x})+c'(\mathbf{x},t),\ \mathbf{x}\in\mathbb{R}^3 \tag{4}$$

where the time average concentration is defined by the following equation:

$$\overline{c}(\mathbf{x}) = \lim_{T\to\infty} \frac{1}{T} \int_{t}^{t+T} c(\mathbf{x},\tau)\mathrm{d}\tau \tag{5}$$

and $c'(\mathbf{x},t)$ is the fluctuating concentration. We replace the time average by the approximation:

$$\overline{c}(\mathbf{x}) = \frac{1}{t_{ref}} \int_{t}^{t+t_{ref}} c(\mathbf{x},t)\mathrm{d}\tau \tag{6}$$

Being interested in the long-term average behavior of diffusion phenomenon, after substituting the Reynolds decomposition, a time average is taken into account. Considering the time-average mass flux in the x - direction:

$$\overline{uc} = \overline{(\overline{u}+u')(\overline{c}+c')} = \overline{\overline{u}\overline{c} + \overline{u}c' + u'\overline{c} + u'c'} \tag{7}$$

where $\overline{c}$ is the average fluctuation velocity.

Applying the formula (6), the average of the fluctuating properties becomes $\overline{u'} = \overline{c'} = 0$, and thus $\overline{uc} = \overline{u}\,\overline{c} + \overline{u'c'}$, where $\overline{\overline{c}} = \overline{c}$.

In order to substitute the Reynolds decomposition into the governing advection-diffusion equation, the first step is to integrate over the integral time scale t_{ref}.

$$\frac{1}{t_{ref}} \int_{t}^{t+t_{ref}} \left[\frac{\partial(\overline{c}+c')}{\partial\tau} + \frac{\partial\left[(\overline{u}_i+u_i')(\overline{c}+c')\right]}{\partial x_i} \right] \mathrm{d}\tau = \frac{1}{t_{ref}} \int_{t}^{t+t_{ref}} \frac{\partial}{\partial x_i}\left[K_m \frac{\partial(\overline{c}+c')}{\partial x_i} \right] \mathrm{d}\tau \tag{8}$$

Moving the terms in $\overline{u_i'c'}$ to the right side, the left becomes:

$$\frac{\partial\overline{c}}{\partial t} + \overline{u}_i \frac{\partial\overline{c}}{\partial x_i} = \frac{\partial\overline{c}}{\partial x_i}\left(K_m \frac{\partial\overline{c}}{\partial x_i} \right) - \frac{\partial\overline{u_i'c'}}{\partial x_i} \tag{9}$$

The unsteady term for the mean concentration (first term on the LHS) has been retained even though it can be set zero according to Eq.(6). Retaining this term is thus not needed for physical reasons, but is instead included to allow the PDE to be conveniently solved with a time-marching scheme.

A model is needed for $\overline{u_i'c'}$, which is a fluctuating mass flux (mass flux associated with the turbulence). The turbulent component is qualitatively described as a form of rapid mixing (molecular diffusion analogy).

The average turbulent diffusion time scale is $\Delta t = t_{ref}$, and the average turbulent diffusion length scale is $\Delta x = u_{ref} t_{ref} = l_{ref}$. The model becomes valid for $t > t_{ref}$. Applying a gradient law to turbulent diffusion phenomenon, it results the following:

$$\overline{u_i'c'} = K_{t,i}\frac{\partial \overline{c}}{\partial x_i} \tag{10},$$

where $K_{t,i}$ is the turbulent diffusion transport coefficient.

Substituting the average turbulent diffusive transport and dropping the over-bar notation, it follows that:

$$\frac{\partial c}{\partial t} + u_i\frac{\partial c}{\partial x_i} = \frac{\partial c}{\partial x_i}\left[\left(K_{t,i} + K_{m,i}\right)\frac{\partial c}{\partial x_i}\right] \tag{11}$$

In the previous equation, t index states for turbulence and m for molecular. Usually, $K_t >> K_m$ and so it becomes:

$$\frac{\partial c}{\partial t} + u_i\frac{\partial c}{\partial x_i} = K_{t,i}\frac{\partial^2 c}{\partial x_i^2} \tag{12}$$

Or, in 3-dimension extended form, the advection-diffusion equation on an arbitrary domain $\Omega \in \mathbb{R}^3$ is given by:

$$\begin{aligned}
&\frac{\partial c}{\partial t} + u\frac{\partial c}{\partial x} + v\frac{\partial c}{\partial y} + w\frac{\partial c}{\partial z} = K_x\frac{\partial^2 c}{\partial x^2} + K_y\frac{\partial^2 c}{\partial y^2} + K_z\frac{\partial^2 c}{\partial z^2}, \mathbf{x} \in \Omega,\ t > 0\\
&c(\mathbf{x},0) = C_0(\mathbf{x}), \mathbf{x} \in \Omega\\
&C(t,\mathbf{x}) = C_{\partial\Omega}(t,\mathbf{x}),\ \mathbf{x} \in \partial\Omega:\ \left(\mathbf{v},\mathbf{n}\right) < 0\\
&\frac{\partial C}{\partial n}(t,\partial\Omega) = 0, \mathbf{x} \in \partial\Omega:\ \left(\mathbf{v},\mathbf{n}\right) \geq 0
\end{aligned} \tag{13}$$

where: $c(x,y,z)$–SO_2 concentration in point of (x,y,z) coordinates at time t;

u, v, w – wind components;

K_x, K_y, K_z – diffusion coefficients (turbulent or molecular diffusion coefficient).

The dispersion eq. (13) is accompanied with initial and boundary conditions, which can depend on specific problem. Here, $\partial\Omega$ is lateral boundary of a certain domain Ω.

In order to solve the above-mentioned time-dependent partial differential equation, the non-dimensional form was obtained with the aid of the following functions:

Non-dimensional time: $\bar{t} = \frac{t}{T}$, where t – current time, T – characteristic time;

Non-dimensional space variable on x-axis: $\bar{x} = \frac{x}{x_{\max}}$, where x – current space, $x_{\max}$ – characteristic longitudinal variable ;

Non-dimensional space variable on y-axis: $\overline{y} = \frac{y}{y_{\max}}$, where y – current variable, $y_{\max}$ – characteristic length ;

Non-dimensional space variable on z-axis: $\overline{z} = \frac{z}{z_{\max}}$, where z – current space on $0z$, $z_{\max}$ – maximum height;

Non-dimensional concentration: $\overline{c} = \frac{c}{c_{\max}}$, where c – current concentration, $c_{\max}$ – maximum concentration admitted by law (10 mg/m^3 air).

The equation below is obtained:

$$\frac{c_{\max}}{T}\cdot\frac{\partial \overline{c}}{\partial \overline{t}} + \frac{c_{\max}}{x_{\max}}u\frac{\partial \overline{c}}{\partial \overline{x}} + \frac{c_{\max}}{y_{\max}}v\frac{\partial \overline{c}}{\partial \overline{y}} + \frac{c_{\max}}{z_{\max}}w\frac{\partial \overline{c}}{\partial \overline{z}} = K_x\frac{c_{\max}}{x_{\max}^2}\frac{\partial^2 \overline{c}}{\partial \overline{x}^2} + K_y\frac{c_{\max}}{y_{\max}^2}\frac{\partial^2 \overline{c}}{\partial \overline{y}^2} + K_z\frac{c_{\max}}{z_{\max}^2}\frac{\partial^2 \overline{c}}{\partial \overline{z}^2} \quad (14)$$

$$\Rightarrow \frac{\partial \overline{c}}{\partial \overline{t}} + \frac{\partial \overline{c}}{\partial \overline{x}} + \frac{v}{u}\frac{x_{\max}}{y_{max}}\frac{\partial \overline{c}}{\partial \overline{y}} + \frac{w}{u}\frac{x_{\max}}{z_{max}}\frac{\partial \overline{c}}{\partial \overline{z}} = \frac{K_x\cdot T}{x_{\max}^2}\frac{\partial^2 \overline{c}}{\partial \overline{x}^2} + \frac{K_y\cdot T}{y_{\max}^2}\frac{\partial^2 \overline{c}}{\partial \overline{y}^2} + \frac{K_z\cdot T}{z_{\max}^2}\frac{\partial^2 \overline{c}}{\partial \overline{z}^2} \quad (15)$$

As $\frac{T\cdot u}{x_{\max}} = \overline{u}$; $\frac{T\cdot v}{z_{\max}} = \overline{v}$; $\frac{K_x\cdot T}{x_{\max}^2} = \overline{K}_x$; $\frac{K_z\cdot T}{z_{\max}^2} = \overline{K}_z$, it follows that:

$$\frac{\partial \overline{c}}{\partial \overline{t}} + \overline{u}\frac{\partial \overline{c}}{\partial \overline{x}} + \overline{v}\frac{\partial \overline{c}}{\partial \overline{y}} + \overline{w}\frac{\partial \overline{c}}{\partial \overline{z}} = \overline{K}_x\frac{\partial^2 \overline{c}}{\partial \overline{x}^2} + \overline{K}_y\frac{\partial^2 \overline{c}}{\partial \overline{y}^2} + \overline{K}_z\frac{\partial^2 \overline{c}}{\partial \overline{z}^2} \quad (16)$$

In what follows the over-bar notation will be dropped and the computation will be performed in non-dimensional form.

3. The numerical scheme

The purpose of this paper is to determine the maximum SO_2 concentration at ground level and the distance, on wind direction, at which SO_2 ground concentration is maximum. The initial data is given in Table 1.

Meteorological conditions for horizontal convection (wind advection) is higher than vertical and lateral convection and therefore it results that:

$$v\frac{\partial c}{\partial y}, w\frac{\partial c}{\partial z} << u\frac{\partial c}{\partial x} ; \quad (17)$$

In order to avoid ground level boundary conditions, for a continuous point source at high $h_d = h$ on $0z$, a second virtual, symmetrical source was imagined, and the boundary condition (13') is replaced by a more convenient condition for the numerical point of view:

$$\frac{\partial c}{\partial z}(x,y,-\infty,t)=0,(x,y)\in(0,\infty)\times\mathbb{R}; \tag{13'}$$

Table 1

Calculus data

Technical characteristic	Value
Fuel flow B [kg/h]	2304
Sulfur mass fraction in fuel s	0.01
Funnel top quote h_c [m]	45
Inner funnel diameter D [m]	1.5
Combustion gas speed at top funnel w [m/s]	8.604
Wind speed at 10 m altitude w_{10} [m/s]	2.5
Maximum concentration admitted (mg/m^3 air).	10
Turbulence index for stable state atmosphere n	0.25

Neglecting terms from (14), the mathematical formulation becomes:

$$\begin{aligned}
&\frac{\partial c}{\partial t}+u\frac{\partial c}{\partial x}=K_x\frac{\partial^2 c}{\partial x^2}+K_y\frac{\partial^2 c}{\partial y^2}+K_z\frac{\partial^2 c}{\partial z^2},(x,y,z)\in(0,\infty)\times\mathbb{R}^2,t>0\\
&c(x,y,z,0)=c_0,\ (x,y,z)\in(0,\infty)\times\mathbb{R}^2\\
&c(0,0,z,t)=\begin{cases}\dfrac{Q_{SO_2}}{uA},z=\pm h\\ 0,z\neq\pm h\end{cases}\\
&\frac{\partial c}{\partial x}(\pm\infty,y,z,,t)=0,(y,z)\in\mathbb{R}^2\\
&\frac{\partial c}{\partial y}(x,\pm\infty,z,t)=0,(x,z)\in(0,\infty)\times\mathbb{R}\\
&\frac{\partial c}{\partial z}(x,y,\pm\infty,t)=0,(x,y)\in(0,\infty)\times\mathbb{R}
\end{aligned} \tag{18}$$

where c_0 is the initial SO_2 concentration, A is the evacuation surface area of the furnace, with diameter D.

3.1. 2D-Formulation

For different boundary conditions and values of u, K_x, K_y, K_z, time dependent solutions for arbitrary parameters are still unknown. For further simplification, a uniform evolution is assumed for concentration along $0y$, so that diffusion on this axis is eliminated, leading to the following equation:

$$\begin{aligned}
&\frac{\partial c}{\partial t}+u\frac{\partial c}{\partial x}=K_x\frac{\partial^2 c}{\partial x^2}+K_z\frac{\partial^2 c}{\partial z^2}\\
&c(x,z,0)=c_{init}\left(x,z\right),\ \left(x,z\right)\in\left(0,\infty\right)\times\mathbb{R}\\
&c(0,z,t)=\begin{cases}\dfrac{Q_{SO_2}}{uA},z=\pm h\\ 0,z\neq\pm h\end{cases}\\
&\frac{\partial c}{\partial x}(\infty,z,t)=0,\ z\in\mathbb{R}\\
&\frac{\partial c}{\partial z}(x,\pm\infty,t)=0,x\in\left(0,\infty\right)
\end{aligned}\tag{19}$$

We assume that the wind speed u and the diffusion coefficients K_x, K_z are constant.

The problem written on infinite domain is replaced by a non-dimensional problem with finite boundaries such that:

$$\begin{aligned}
&\frac{\partial c}{\partial t}+u\frac{\partial c}{\partial x}=K_x\frac{\partial^2 c}{\partial x^2}+K_z\frac{\partial^2 c}{\partial z^2},\left(x,z\right)\in\left(0,1\right)\times\left(-1,1\right),t>0\\
&c(x,z,0)=c_{init}\left(x,z\right)/c_{\max},\ \left(x,z\right)\in\left[0,1\right]\times\left[-1,1\right]\\
&c(0,z,t)=\begin{cases}\dfrac{Q_{SO_2}}{uAc_{\max}},z=\pm h_d/z_{\max}\\ 0,z\neq\pm h_d/z_{\max},z\in\left[-1,1\right]\end{cases}\\
&\left(\frac{\partial c}{\partial t}+u\frac{\partial c}{\partial x}\right)(1,z,t)=0,\ z\in\left[-1,1\right]\\
&\frac{\partial c}{\partial z}(x,\pm1,t)=0,\ x\in\left[0,1\right]
\end{aligned}\tag{20}$$

The choice of the lateral boundary conditions is important to avoid absorption or reflection from these boundaries. Therefore, at the lateral boundaries, no advection and diffusion flux was assumed (zero gradients). For outgoing boundary, the flow was assumed free of diffusion whereas for ingoing flux, null concentrations were set, except only the issuing source point.

3.2. Spatial scheme

In this work, a first-order explicit upwind numerical scheme was used for interior points and for the boundary the classical asymmetric schemes of increasing order starting with first node up to the fifth node.

The diffusion terms are evaluated using tenth order schemes. The spatial derivative $c_{i,xx}$ for the boundaries can be approximated using Taylor expansions by 12 -point stencil:

$$\left.\frac{\partial^2 c}{\partial x^2}\right|_i = \frac{1}{\Delta x^2}\sum_{j=-L}^{R}\alpha_{i+j}c_{i+j} \tag{21}$$

where Δx is the spacing of uniform mesh. The above formula involves $R+L+1$ constants (i.e. the sum between the order of finite-difference scheme and the order of derivative).

Table 2

Coefficients of boundary schemes for second derivative at the boundary nodes (1-5)

α_i	(Node 1) $R=11;\ L=0$	(Node 2) $R=10;\ L=1$	(Node 3) $R=9;\ L=2$	(Node 4) $R=8;\ L=3$	(Node 5) $R=7;\ L=4$
c_i	190553/25200.	671./1260.	-419./12600.	31./6300.	-29./25200.
c_{i+1}	-55991/1260	29513./25200.	5869./6300.	-1163./12600.	59./3150.
c_{i+2}	69851/504	-2341./252.	-737./720.	1583./1260.	-53./315.
c_{i+3}	-74471/252	3601./168.	-829./420.	-2123./1008.	-317./210.
c_{i+4}	76781./168.	-4021./126.	2089./420.	97./210.	-6743./2520.
c_{i+5}	-78167./150.	4231./120.	-2509./450.	323./300.	103./75.
c_{i+6}	79091./180.	-4357./150.	2719./600.	-463./450.;	1./75.
c_{i+7}	-11393./42.	4441./252.	-569./210.	533./840.	-37./315.
c_{i+8}	40123./336.	-643./84.	2929./2520.	-23./84.	109./1680.
c_{i+9}	-8959./252.	2273./1008.	-61./180.	67./840.	-13./630.
c_{i+10}	80939./12600.	-509./1260.	1517./25200.	-89./6300.	2./525.
c_{i+11}	-671./1260.	419./12600.	-31./6300.	29./25200.	-1./3150.

For interior points the expression of the scheme is symmetric ($R=L$).

Table 3

Coefficients of interior schemes for second derivative

α_i (Node i) $R=5;\ L=5$	c_i
1./3150	c_{i-5}
-5./1008	c_{i-4}
5./126	c_{i-3}
-5./21	c_{i-2}
5./3	c_{i-1}
-5269./1800	c_i
5./3	c_{i+1}
-5./21	c_{i+2}
5./126	c_{i+3}
-5./1008	c_{i+4}
1./3150	c_{i+5}

3.3. Temporal scheme

After the application of the finite differences schemes to equation (16), the expression can be reduced to a set of ordinary differential equations in time. Then the governing equation becomes:

$$\begin{aligned} &\frac{d\mathbf{c}}{dt} = L(\mathbf{c}),\ t \in \left(t^n, t^{n+1}\right) \\ &\mathbf{c}\left(t^n\right) = \mathbf{c}^n \end{aligned} \tag{22}$$

where L indicates a spatial differential operator and $\mathbf{c}^n = \left(c_0^n, c_1^n, ..., c_N^n\right)$. Each spatial derivative on the right hand side of equation (19) was computed using the present schemes and then the semi-discrete equation (19) was solved using a particularly simple Runge-Kutta time integrator introduced by Jameson-Schmidt-Turkel:

$$\begin{aligned} &\mathbf{c}_0 = \mathbf{c}^n \\ &\mathbf{c}_i = \mathbf{c}^n + \frac{dt}{5-i} L\left(\mathbf{c}_{i-1}\right), i = 1,4 \\ &\mathbf{c}^{n+1} = \mathbf{c}_4 \end{aligned} \tag{23}$$

4. Numerical results

We chose the following characteristic quantities: $x_{\max} = 8000\,m$, $h_d = 53\,m$, $z_{\max} = 4h_d$, $T = x_{\max}/u$. The simulation time is $t_{final} = 5400\,s$. The computational domain in non-dimensional formulation was discretized by a 100×100 grid. The initial SO_2 concentration and the maximum concentration admitted are $c_0 = 17 \cdot 10^{-3}\,mg/m^3 air$ and $c_{\max} = 10\,mg/m^3 air$.

The considered diffusion coefficients are $K_x = K_z = 0.115$. We propose the following function for the initial sulpfur dioxide concentration:

$$c_{init}(x,z) = c_{SO_2}/c_{\max} e^{-5000.[(x-x_0)^2+(y-y_0)^2]} + c_0/c_{\max} \tag{24}$$

where

$$c_{SO_2} = \frac{Q_{SO_2}}{u\left(\pi D^2/4\right)} \tag{25}$$

and $Q_{SO_2} = 0.0128\,kg/s$ is the mass flow rate, $u = 2.5\ m/s$, the horizontal wind velocity and $D = 1.5\,m$ the inner furnace diameter at the top.

Figs. 4-5 show 2D-evolution of SO_2 concentration for 5400 s due to a continuous source point. After 4000s the concentration in the entire domain is stabilized. As mentioned before, the scope of this paper is to correctly estimate the ground concentration, as well as its subsequent transmission through the atmosphere. In figs.6-7 the simulations show that the profile of the concentration is an increasing curve and becomes stable in each point after a specific period of time.

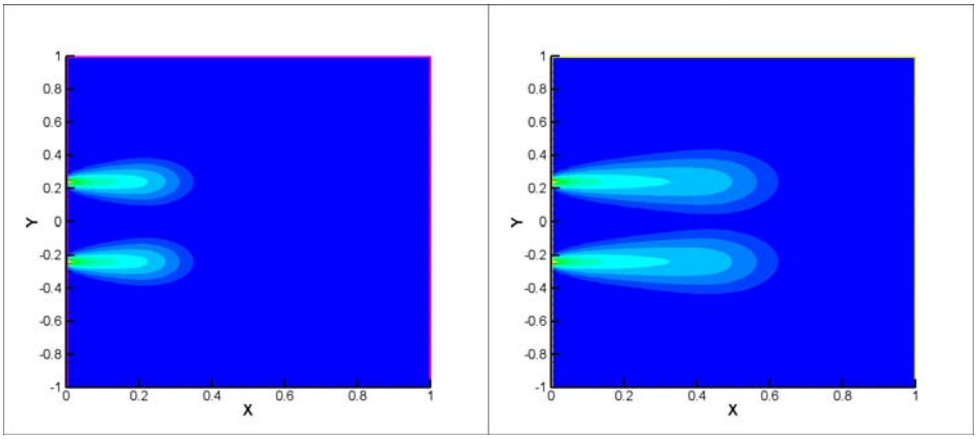

Fig.4. SO_2 concentration at t = 800 s and t = 1600 s

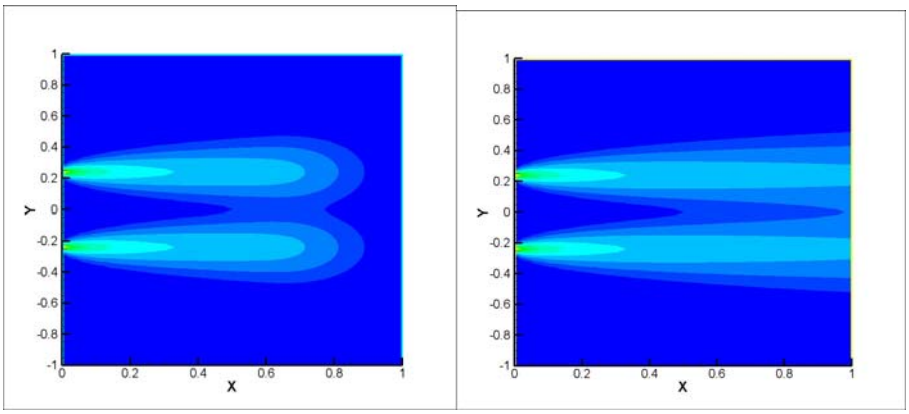

Fig.5. SO_2 concentration at t = 2400 and t= 5400 s

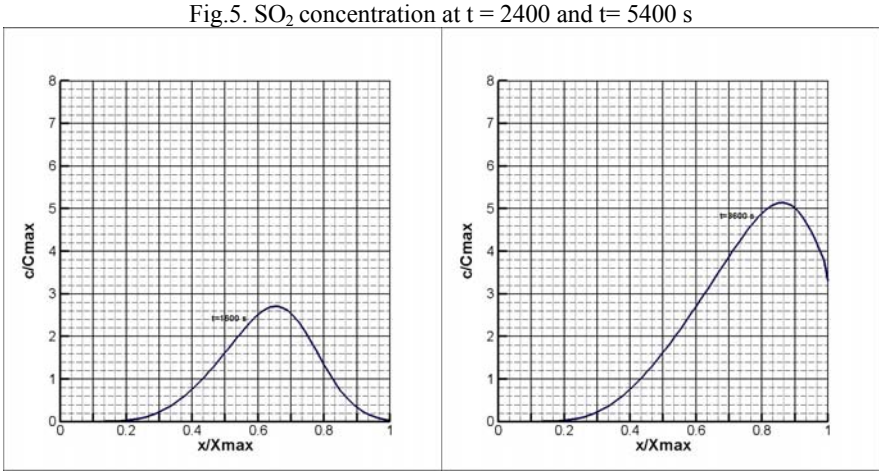

Fig.6. Concentration profile at t=1600s and t=2400s

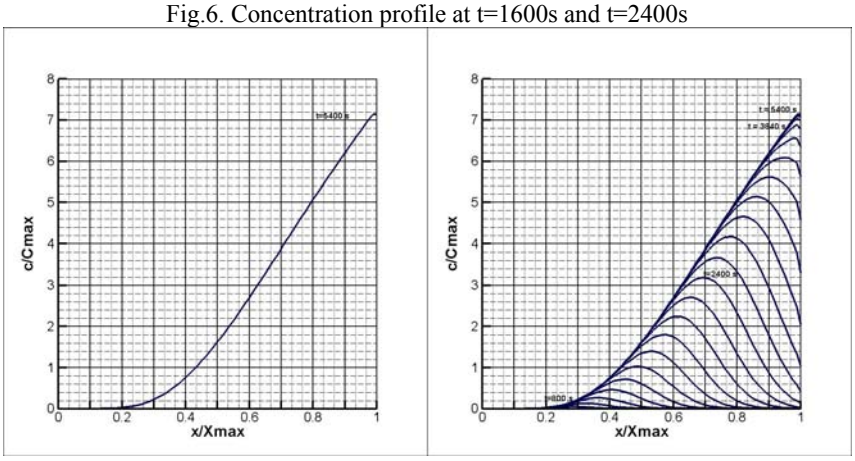

Fig.7. Stabilized curve shape at t=5400s and the entire evolution of the concentration of SO_2 at the ground

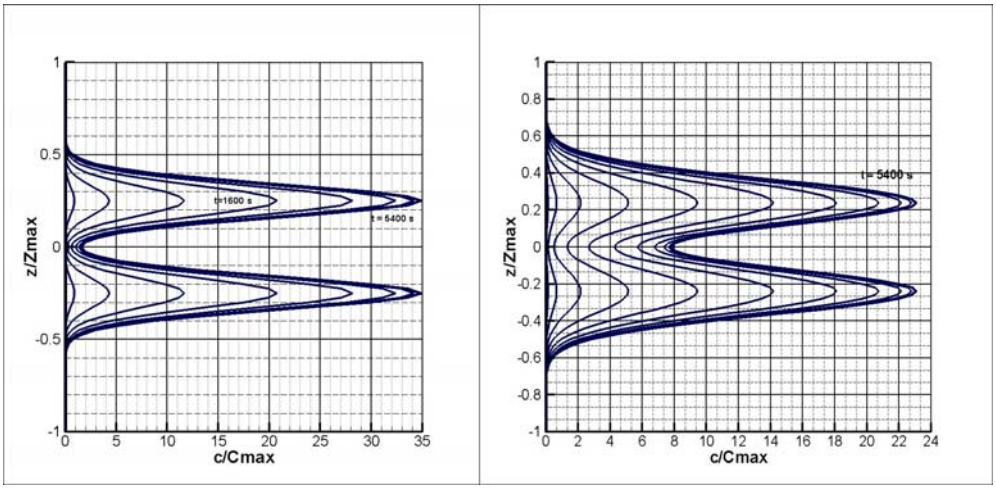

Fig.8. Concentration profile at a fixed point x/x_{max}=0.5 and x/x_{max}=0.98

5. Conclusions

SO_2 dispersion from flue gas was well simulated by using Reynolds decomposition for turbulent advection-diffusion equation substituted into the classical form, average time scale, for a continuous point source, while imaging a second virtual asymmetrical source. Numerical scheme involved first-order upwind method for interior points and asymmetric scheme of increasing order starting with first node up to the fifth node for the boundary.

Two -dimensional simulation for SO_2 emission from a continuous source point revealed stabilization in the entire domain. Concentration profiles are increasing curves which become stable in each point after a specific period of time. Therefore, it can be concluded that the present approach correctly estimates the SO_2 ground concentration, as well as its subsequent transmission through the atmosphere.

R E F E R E N C E S

[1] *Sigal Gottlieb, Lee-Ad J. Gottlieb*, Strong Stability Preserving Properties of Runge-Kutta Time Discretization Methods for Linear Constant Coefficient Operators, Journal of Scientific Computing, vol.18, no.1, Feb.2003, pp. 83-109

[2] *Sanjiva K. Lele*, Compact Finite Difference Schemes with Spectral-like Resolution, Journal of Computational Physics, vol.103, 1992, pp. 16-42

[3] *Dumitru Dobrinescu*, Procese de transfer termic si utilaje specifice, (Thermal Transfer Processes and Specific Equipment) Ed. Didactica si Pedagocica, Bucuresti, 1983, pp. 449-465

[4] *Antonion Costa, Giovanni Macedonio, Giovanni Chiodini*, Numerical Model of Gas Dispersion Emitted from Volcanic Sources, Annals of Geopghysics, vol.48, no.4/5, Aug/Oct. 2005, pp. 805-815
[5] *Scott A. Socolofsky, Gerhard H. Jirka*, Special Topics in Mixing and Transport Processes in the Environment, 5th Ed., Texas A&M University, 2005, pp. 55-56
[6] *Montri Thangmoon*, Numerical Experiment of Air Pollution Concentration in the Street Tunnel, International Mathematical Forum, vol. 5, no. 10, 2010, pp. 449-465
[7] *M. Thangmoon, R. McKibbin*, A Comparison of Some Numerical Methods for the Advection-Diffusion Equation, Res.Lett.Inf.Math.Sci., vol. 10, 2006, pp. 49-62
[8] *Klaus A. Hoffmann, Steve T. Chiang,* Computational Fluid Dynamics, Vol. 3, 2000, pp.117-138.
[9] *C. Bogey, C. Bailly,* Three-dimensional non-reflective boundary conditions for acoustic simulations: far field formulation and validation test cases, Acta Acustica, Vol. 88, No. 4, 2002, pp. 463–471.
[10] *Murat Sari, Gürhan Güraslan and Asuman Zeytinoğlu*, High-order finite difference schemes for solving the advection-diffusion equation, Mathematical and Computational Applications, Vol. 15, No. 3, 2010, pp. 449-460.
[11] *J. Li*, High-order finite difference schemes for differential equations containing higher derivatives, Applied Mathematics and Computation, 171, 2005, pp. 1157-1176.
[12] *J. Geiser*, Stability of Iterative Operator-Splitting Methods, International Journal of Computer Mathematics, Volume 87, Issue 8, 2010, pp. 1857-1871.